

Search for Kaluza-Klein Graviton Emission in $p\bar{p}$ Collisions at $\sqrt{s} = 1.8$ TeV using the Missing Energy Signature

The CDF Collaboration

- D. Acosta,¹⁴ T. Affolder,⁷ H. Akimoto,⁵¹ M.G. Albrow,¹³ D. Ambrose,³⁷ D. Amidei,²⁸ K. Anikeev,²⁷
 J. Antos,¹ G. Apollinari,¹³ T. Arisawa,⁵¹ A. Artikov,¹¹ T. Asakawa,⁴⁹ W. Ashmanskas,² F. Azfar,³⁵
 P. Azzi-Bacchetta,³⁶ N. Bacchetta,³⁶ H. Bachacou,²⁵ W. Badgett,¹³ S. Bailey,¹⁸ P. de Barbaro,⁴¹
 A. Barbaro-Galtieri,²⁵ V.E. Barnes,⁴⁰ B.A. Barnett,²¹ S. Baroiant,⁵ M. Barone,¹⁵ G. Bauer,²⁷ F. Bedeschi,³⁸
 S. Behari,²¹ S. Belforte,⁴⁸ W.H. Bell,¹⁷ G. Bellettini,³⁸ J. Bellinger,⁵² D. Benjamin,¹² J. Bensinger,⁴
 A. Beretvas,¹³ J. Berryhill,¹⁰ A. Bhatti,⁴² M. Binkley,¹³ D. Bisello,³⁶ M. Bishai,¹³ R.E. Blair,² C. Blocker,⁴
 K. Bloom,²⁸ B. Blumenfeld,²¹ S.R. Blusk,⁴¹ A. Bocci,⁴² A. Bodek,⁴¹ G. Bolla,⁴⁰ A. Bolshov,²⁷ Y. Bonushkin,⁶
 D. Bortoletto,⁴⁰ J. Boudreau,³⁹ A. Brandl,³¹ C. Bromberg,²⁹ M. Brozovic,¹² E. Brubaker,²⁵ N. Bruner,³¹
 J. Budagov,¹¹ H.S. Budd,⁴¹ K. Burkett,¹⁸ G. Busetto,³⁶ K.L. Byrum,² S. Cabrera,¹² P. Calafiura,²⁵
 M. Campbell,²⁸ W. Carithers,²⁵ J. Carlson,²⁸ D. Carlsmith,⁵² W. Caskey,⁵ A. Castro,³ D. Cauz,⁴⁸ A. Cerri,²⁵
 L. Cerrito,²⁰ A.W. Chan,¹ P.S. Chang,¹ P.T. Chang,¹ J. Chapman,²⁸ C. Chen,³⁷ Y.C. Chen,¹ M.-T. Cheng,¹
 M. Chertok,⁵ G. Chiarelli,³⁸ I. Chirikov-Zorin,¹¹ G. Chlachidze,¹¹ F. Chlebana,¹³ L. Christofek,²⁰ M.L. Chu,¹
 J.Y. Chung,³³ W.-H. Chung,⁵² Y.S. Chung,⁴¹ C.I. Ciobanu,³³ A.G. Clark,¹⁶ M. Coca,⁴¹ A. Connolly,²⁵
 M. Convery,⁴² J. Conway,⁴⁴ M. Cordelli,¹⁵ J. Cranshaw,⁴⁶ R. Culbertson,¹³ D. Dagenhart,⁴ S. D'Auria,¹⁷
 S. De Cecco,⁴³ F. DeJongh,¹³ S. Dell'Agnello,¹⁵ M. Dell'Orso,³⁸ S. Demers,⁴¹ L. Demortier,⁴² M. Deninno,³
 D. De Pedis,⁴³ P.F. Derwent,¹³ T. Devlin,⁴⁴ C. Dionisi,⁴³ J.R. Dittmann,¹³ A. Dominguez,²⁵
 S. Donati,³⁸ M. D'Onofrio,³⁸ T. Dorigo,³⁶ N. Eddy,²⁰ K. Einsweiler,²⁵ E. Engels, Jr.,³⁹ R. Erbacher,¹³
 D. Errede,²⁰ S. Errede,²⁰ R. Eusebi,⁴¹ Q. Fan,⁴¹ S. Farrington,¹⁷ R.G. Feild,⁵³ J.P. Fernandez,⁴⁰
 C. Ferretti,²⁸ R.D. Field,¹⁴ I. Fiori,³ B. Flaughier,¹³ L.R. Flores-Castillo,³⁹ G.W. Foster,¹³ M. Franklin,¹⁸
 J. Freeman,¹³ J. Friedman,²⁷ Y. Fukui,²³ I. Furic,²⁷ S. Galeotti,³⁸ A. Gallas,³² M. Gallinaro,⁴² T. Gao,³⁷
 M. Garcia-Sciveres,²⁵ A.F. Garfinkel,⁴⁰ P. Gatti,³⁶ C. Gay,⁵³ D.W. Gerdes,²⁸ E. Gerstein,⁹ S. Giagu,⁴³
 P. Giannetti,³⁸ K. Giolo,⁴⁰ M. Giordani,⁵ P. Giromini,¹⁵ V. Glagolev,¹¹ D. Glenzinski,¹³ M. Gold,³¹
 N. Goldschmidt,²⁸ J. Goldstein,¹³ G. Gomez,⁸ M. Goncharov,⁴⁵ I. Gorelov,³¹ A.T. Goshaw,¹² Y. Gotra,³⁹
 K. Goulianios,⁴² C. Green,⁴⁰ A. Gresele,³ G. Grim,⁵ C. Grossi-Pilcher,¹⁰ M. Guenther,⁴⁰ G. Guillian,²⁸
 J. Guimaraes da Costa,¹⁸ R.M. Haas,¹⁴ C. Haber,²⁵ S.R. Hahn,¹³ E. Halkiadakis,⁴¹ C. Hall,¹⁸ T. Handa,¹⁹
 R. Handler,⁵² F. Happacher,¹⁵ K. Hara,⁴⁹ A.D. Hardman,⁴⁰ R.M. Harris,¹³ F. Hartmann,²² K. Hatakeyama,⁴²
 J. Hauser,⁶ J. Heinrich,³⁷ A. Heiss,²² M. Hennecke,²² M. Herndon,²¹ C. Hill,⁷ A. Hocker,⁴¹ K.D. Hoffman,¹⁰
 R. Hollebeek,³⁷ L. Holloway,²⁰ S. Hou,¹ B.T. Huffman,³⁵ R. Hughes,³³ J. Huston,²⁹ J. Huth,¹⁸ H. Ikeda,⁴⁹
 C. Issever,⁷ J. Incandela,⁷ G. Introzzi,³⁸ M. Iori,⁴³ A. Ivanov,⁴¹ J. Iwai,⁵¹ Y. Iwata,¹⁹ B. Iyutin,²⁷ E. James,²⁸
 M. Jones,³⁷ U. Joshi,¹³ H. Kambara,¹⁶ T. Kamon,⁴⁵ T. Kaneko,⁴⁹ J. Kang,²⁸ M. Karagoz Unel,³² K. Karr,⁵⁰
 S. Kartal,¹³ H. Kasha,⁵³ Y. Kato,³⁴ T.A. Keaffaber,⁴⁰ K. Kelley,²⁷ M. Kelly,²⁸ R.D. Kennedy,¹³ R. Kephart,¹³
 D. Khazins,¹² T. Kikuchi,⁴⁹ B. Kilminster,⁴¹ B.J. Kim,²⁴ D.H. Kim,²⁴ H.S. Kim,²⁰ M.J. Kim,⁹ S.B. Kim,²⁴
 S.H. Kim,⁴⁹ T.H. Kim,²⁷ Y.K. Kim,²⁵ M. Kirby,¹² M. Kirk,⁴ L. Kirsch,⁴ S. Klimentko,¹⁴ P. Koehn,³³
 K. Kondo,⁵¹ J. Konigsberg,¹⁴ A. Korn,²⁷ A. Korytov,¹⁴ K. Kotelnikov,³⁰ E. Kovacs,² J. Kroll,³⁷ M. Kruse,¹²
 V. Krutelyov,⁴⁵ S.E. Kuhlmann,² K. Kurino,¹⁹ T. Kuwabara,⁴⁹ N. Kuznetsova,¹³ A.T. Laasanen,⁴⁰
 N. Lai,¹⁰ S. Lami,⁴² S. Lammel,¹³ J. Lancaster,¹² K. Lannon,²⁰ M. Lancaster,²⁶ R. Lander,⁵ A. Lath,⁴⁴
 G. Latino,³¹ T. LeCompte,² Y. Le,²¹ J. Lee,⁴¹ S.W. Lee,⁴⁵ N. Leonardo,²⁷ S. Leone,³⁸ J.D. Lewis,¹³ K. Li,⁵³
 C.S. Lin,¹³ M. Lindgren,⁶ T.M. Liss,²⁰ J.B. Liu,⁴¹ T. Liu,¹³ Y.C. Liu,¹ D.O. Litvintsev,¹³ O. Lobban,⁴⁶
 N.S. Lockyer,³⁷ A. Loginov,³⁰ J. Loken,³⁵ M. Loreti,³⁶ D. Lucchesi,³⁶ P. Lukens,¹³ S. Lusin,⁵² L. Lyons,³⁵
 J. Lys,²⁵ R. Madrak,¹⁸ K. Maeshima,¹³ P. Maksimovic,²¹ L. Malferrari,³ M. Mangano,³⁸ G. Manca,³⁵
 M. Mariotti,³⁶ G. Martignon,³⁶ M. Martin,²¹ A. Martin,⁵³ V. Martin,³² M. Martínez,¹³ J.A.J. Matthews,³¹
 P. Mazzanti,³ K.S. McFarland,⁴¹ P. McIntyre,⁴⁵ M. Menguzzato,³⁶ A. Menzione,³⁸ P. Merkel,¹³
 C. Mesropian,⁴² A. Meyer,¹³ T. Miao,¹³ R. Miller,²⁹ J.S. Miller,²⁸ H. Minato,⁴⁹ S. Miscetti,¹⁵ M. Mishina,²³
 G. Mitselmakher,¹⁴ Y. Miyazaki,³⁴ N. Moggi,³ E. Moore,³¹ R. Moore,²⁸ Y. Morita,²³ T. Moulik,⁴⁰

M. Mulhearn,²⁷ A. Mukherjee,¹³ T. Muller,²² A. Munar,³⁸ P. Murat,¹³ S. Murgia,²⁹ J. Nachtman,⁶
 V. Nagaslaev,⁴⁶ S. Nahn,⁵³ H. Nakada,⁴⁹ I. Nakano,¹⁹ R. Napora,²¹ F. Niell,²⁸ C. Nelson,¹³ T. Nelson,¹³
 C. Neu,³³ M.S. Neubauer,²⁷ D. Neuberger,²² C. Newman-Holmes,¹³ C-Y.P. Ngan,²⁷ T. Nigmanov,³⁹
 H. Niu,⁴ L. Nodulman,² A. Nomerotski,¹⁴ S.H. Oh,¹² Y.D. Oh,²⁴ T. Ohmoto,¹⁹ T. Ohsugi,¹⁹ R. Oishi,⁴⁹
 T. Okusawa,³⁴ J. Olsen,⁵² W. Orejudos,²⁵ C. Pagliarone,³⁸ F. Palmonari,³⁸ R. Paoletti,³⁸ V. Papadimitriou,⁴⁶
 D. Partos,⁴ J. Patrick,¹³ G. Paulette,⁴⁸ M. Paulini,⁹ T. Pauly,³⁵ C. Paus,²⁷ D. Pellett,⁵ A. Penzo,⁴⁸
 L. Pescara,³⁶ T.J. Phillips,¹² G. Piacentino,³⁸ J. Piedra,⁸ K.T. Pitts,²⁰ A. Pompoš,⁴⁰ L. Pondrom,⁵²
 G. Pope,³⁹ T. Pratt,³⁵ F. Prokoshin,¹¹ J. Proudfoot,² F. Ptahos,¹⁵ O. Pukhov,¹¹ G. Punzi,³⁸
 J. Rademacker,³⁵ A. Rakitine,²⁷ F. Ratnikov,⁴⁴ H. Ray,²⁸ D. Reher,²⁵ A. Reichold,³⁵ P. Renton,³⁵
 M. Rescigno,⁴³ A. Ribon,³⁶ W. Riegler,¹⁸ F. Rimondi,³ L. Ristori,³⁸ M. Riveline,⁴⁷ W.J. Robertson,¹²
 T. Rodrigo,⁸ S. Rolli,⁵⁰ L. Rosenson,²⁷ R. Roser,¹³ R. Rossin,³⁶ C. Rott,⁴⁰ A. Roy,⁴⁰ A. Ruiz,⁸ D. Ryan,⁵⁰
 A. Safonov,⁵ R. St. Denis,¹⁷ W.K. Sakamoto,⁴¹ D. Saltzberg,⁶ C. Sanchez,³³ A. Sansoni,¹⁵ L. Santi,⁴⁸
 S. Sarkar,⁴³ H. Sato,⁴⁹ P. Savard,⁴⁷ A. Savoy-Navarro,¹³ P. Schlabach,¹³ E.E. Schmidt,¹³ M.P. Schmidt,⁵³
 M. Schmitt,³² L. Scodellaro,³⁶ A. Scott,⁶ A. Scribano,³⁸ A. Sedov,⁴⁰ S. Seidel,³¹ Y. Seiya,⁴⁹ A. Semenov,¹¹
 F. Semeria,³ T. Shah,²⁷ M.D. Shapiro,²⁵ P.F. Shepard,³⁹ T. Shibayama,⁴⁹ M. Shimojima,⁴⁹ M. Shochet,¹⁰
 A. Sidoti,³⁶ J. Siegrist,²⁵ A. Sill,⁴⁶ P. Sinervo,⁴⁷ P. Singh,²⁰ A.J. Slaughter,⁵³ K. Sliwa,⁵⁰ F.D. Snider,¹³
 R. Snihur,²⁶ A. Solodsky,⁴² T. Speer,¹⁶ M. Spezziga,⁴⁶ P. Sphicas,²⁷ F. Spinella,³⁸ M. Spiropulu,¹⁰
 L. Spiegel,¹³ J. Steele,⁵² A. Stefanini,³⁸ J. Strologas,²⁰ F. Strumia,¹⁶ D. Stuart,⁷ A. Sukhanov,¹⁴
 K. Sumorok,²⁷ T. Suzuki,⁴⁹ T. Takano,³⁴ R. Takashima,¹⁹ K. Takikawa,⁴⁹ P. Tamburello,¹² M. Tanaka,⁴⁹
 B. Tannenbaum,⁶ M. Tecchio,²⁸ R.J. Tesarek,¹³ P.K. Teng,¹ K. Terashi,⁴² S. Tether,²⁷ J. Thom,¹³
 A.S. Thompson,¹⁷ E. Thomson,³³ R. Thurman-Keup,² P. Tipton,⁴¹ S. Tkaczyk,¹³ D. Toback,⁴⁵ K. Tollefson,²⁹
 D. Tonelli,³⁸ M. Tonnesmann,²⁹ H. Toyoda,³⁴ W. Trischuk,⁴⁷ J.F. de Troconiz,¹⁸ J. Tseng,²⁷ D. Tsybychev,¹⁴
 N. Turini,³⁸ F. Ukegawa,⁴⁹ T. Unverhau,¹⁷ T. Vaiciulis,⁴¹ A. Varganov,²⁸ E. Vataga,³⁸ S. Vejcik III,¹³
 G. Velev,¹³ G. Veramendi,²⁵ R. Vidal,¹³ I. Vila,⁸ R. Vilar,⁸ I. Volobouev,²⁵ M. von der Mey,⁶ D. Vucinic,²⁷
 R.G. Wagner,² R.L. Wagner,¹³ W. Wagner,²² Z. Wan,⁴⁴ C. Wang,¹² M.J. Wang,¹ S.M. Wang,¹⁴ B. Ward,¹⁷
 S. Waschke,¹⁷ T. Watanabe,⁴⁹ D. Waters,²⁶ T. Watts,⁴⁴ M. Weber,²⁵ H. Wenzel,²² W.C. Wester III,¹³
 B. Whitehouse,⁵⁰ A.B. Wicklund,² E. Wicklund,¹³ T. Wilkes,⁵ H.H. Williams,³⁷ P. Wilson,¹³ B.L. Winer,³³
 D. Winn,²⁸ S. Wolbers,¹³ D. Wolinski,²⁸ J. Wolinski,²⁹ S. Wolinski,²⁸ M. Wolter,⁵⁰ S. Worm,⁴⁴ X. Wu,¹⁶
 F. Würthwein,²⁷ J. Wyss,³⁸ U.K. Yang,¹⁰ W. Yao,²⁵ G.P. Yeh,¹³ P. Yeh,¹ K. Yi,²¹ J. Yoh,¹³ C. Yosef,²⁹
 T. Yoshida,³⁴ I. Yu,²⁴ S. Yu,³⁷ Z. Yu,⁵³ J.C. Yun,¹³ L. Zanello,⁴³ A. Zanetti,⁴⁸ F. Zetti,²⁵ and S. Zucchelli³¹

¹ ¹ Institute of Physics, Academia Sinica, Taipei, Taiwan 11529, Republic of China

² Argonne National Laboratory, Argonne, Illinois 60439

³ Istituto Nazionale di Fisica Nucleare, University of Bologna, I-40127 Bologna, Italy

⁴ Brandeis University, Waltham, Massachusetts 02254

⁵ University of California at Davis, Davis, California 95616

⁶ University of California at Los Angeles, Los Angeles, California 90024

⁷ University of California at Santa Barbara, Santa Barbara, California 93106

⁸ Instituto de Fisica de Cantabria, CSIC-University of Cantabria, 39005 Santander, Spain

⁹ Carnegie Mellon University, Pittsburgh, Pennsylvania 15213

¹⁰ Enrico Fermi Institute, University of Chicago, Chicago, Illinois 60637

¹¹ Joint Institute for Nuclear Research, RU-141980 Dubna, Russia

¹² Duke University, Durham, North Carolina 27708

¹³ Fermi National Accelerator Laboratory, Batavia, Illinois 60510

¹⁴ University of Florida, Gainesville, Florida 32611

¹⁵ Laboratori Nazionali di Frascati, Istituto Nazionale di Fisica Nucleare, I-00044 Frascati, Italy

¹⁶ University of Geneva, CH-1211 Geneva 4, Switzerland

¹⁷ Glasgow University, Glasgow G12 8QQ, United Kingdom

¹⁸ Harvard University, Cambridge, Massachusetts 02138

¹⁹ Hiroshima University, Higashi-Hiroshima 724, Japan

²⁰ University of Illinois, Urbana, Illinois 61801

²¹ The Johns Hopkins University, Baltimore, Maryland 21218

²² Institut für Experimentelle Kernphysik, Universität Karlsruhe, 76128 Karlsruhe, Germany

²³ High Energy Accelerator Research Organization (KEK), Tsukuba, Ibaraki 305, Japan

²⁴ Center for High Energy Physics: Kyungpook National University, Taegu 702-701; Seoul National University, Seoul 151-742; and SungKyunKwan University, Suwon 440-746; Korea

²⁵ Ernest Orlando Lawrence Berkeley National Laboratory, Berkeley, California 94720

²⁶ University College London, London WC1E 6BT, United Kingdom

²⁷ Massachusetts Institute of Technology, Cambridge, Massachusetts 02139

- ²⁸ University of Michigan, Ann Arbor, Michigan 48109
²⁹ Michigan State University, East Lansing, Michigan 48824
³⁰ Institution for Theoretical and Experimental Physics, ITEP, Moscow 117259, Russia
³¹ University of New Mexico, Albuquerque, New Mexico 87131
³² Northwestern University, Evanston, Illinois 60208
³³ The Ohio State University, Columbus, Ohio 43210
³⁴ Osaka City University, Osaka 588, Japan
³⁵ University of Oxford, Oxford OX1 3RH, United Kingdom
³⁶ Universita di Padova, Istituto Nazionale di Fisica Nucleare, Sezione di Padova, I-35131 Padova, Italy
³⁷ University of Pennsylvania, Philadelphia, Pennsylvania 19104
³⁸ Istituto Nazionale di Fisica Nucleare, University and Scuola Normale Superiore of Pisa, I-56100 Pisa, Italy
³⁹ University of Pittsburgh, Pittsburgh, Pennsylvania 15260
⁴⁰ Purdue University, West Lafayette, Indiana 47907
⁴¹ University of Rochester, Rochester, New York 14627
⁴² Rockefeller University, New York, New York 10021
⁴³ Istituto Nazionale de Fisica Nucleare, Sezione di Roma, University di Roma I, "La Sapienza," I-00185 Roma, Italy
⁴⁴ Rutgers University, Piscataway, New Jersey 08855
⁴⁵ Texas A&M University, College Station, Texas 77843
⁴⁶ Texas Tech University, Lubbock, Texas 79409
⁴⁷ Institute of Particle Physics, University of Toronto, Toronto M5S 1A7, Canada
⁴⁸ Istituto Nazionale di Fisica Nucleare, University of Trieste/ Udine, Italy
⁴⁹ University of Tsukuba, Tsukuba, Ibaraki 305, Japan
⁵⁰ Tufts University, Medford, Massachusetts 02155
⁵¹ Waseda University, Tokyo 169, Japan
⁵² University of Wisconsin, Madison, Wisconsin 53706
⁵³ Yale University, New Haven, Connecticut 06520

(Dated: Sept 15 2003)

We report on a search for direct Kaluza-Klein graviton production in a data sample of 84 pb^{-1} of $p\bar{p}$ collisions at $\sqrt{s} = 1.8 \text{ TeV}$, recorded by the Collider Detector at Fermilab. We investigate the final state of large missing transverse energy and one or two high energy jets. We compare the data with the predictions from a $3 + 1 + n$ -dimensional Kaluza-Klein scenario in which gravity becomes strong at the TeV scale. At 95% confidence level (C.L.) for $n = 2, 4$, and 6 we exclude an effective Planck scale below $1.0, 0.77$, and 0.71 TeV , respectively.

PACS numbers: 14.80.-j, 12.10.-g, 13.85.Rm

Early attempts to unify gravity and electromagnetism led to the idea of an extra circular spatial dimension [1]. Because of the periodicity of the extra dimension, the metric field of the five-dimensional spacetime is Fourier expandable in the extra dimension with four-dimensional fields (called Kaluza-Klein (KK) modes) as coefficients.

More recently, Kaluza-Klein theories appear in scenarios of large extra dimensions as introduced by Arkani-Hamed, Dimopoulos, and Dvali (ADD) [2]. In these theories the standard model gauge theory is confined to a 3-dimensional domain wall (brane), embedded in a higher dimensional compactified bulk space. Only gravity propagates in the full bulk space. The n compactified extra dimensions are assumed for simplicity to be "large" circles of common circumference R (an n -torus). As a result of compactification, the gravitational field that propagates in the bulk can be expanded in a series of states known collectively as the graviton KK tower. Similar to a particle in a box, the momentum of the bulk field is quantized in the compactified dimensions. For an observer trapped on the brane, each quantum of momentum in the com-

pactified volume appears as a KK excited state with mass $m^2 = \vec{p}_n^2$, where \vec{p}_n is the momentum in the compactified dimensions, and with identical spin and gauge numbers.

In such a model the Planck scale M_{Pl} , the radius R of the compactified space (here assumed to be a torus), and the new effective Planck scale M_D are related by [3]

$$M_{Pl}^2 = 8\pi R^n M_D^{2+n},$$

where n is the number of extra dimensions. If M_D takes values as low as a few TeV the Higgs naturalness problem [4] of the standard model can be solved by introducing a cutoff not too far above the electroweak scale with new physics entering at energies above this cutoff. The hierarchy problem of the standard model is also recast: the question of why M_{Pl} is so large compared to the Z boson mass (M_Z) is replaced with the question of why R is so large compared to $1/M_Z$, and an ultraviolet hierarchy problem is replaced with an infrared one. If we take the most optimistic case of $M_D = 1 \text{ TeV}$ and use $M_{Pl} \sim 10^{19} \text{ GeV}$, we find that for $n = 1, 2, 4$ and 6 , $R \sim 10^{11} \text{ m}, 1 \text{ mm}, 10 \text{ nm}$ and

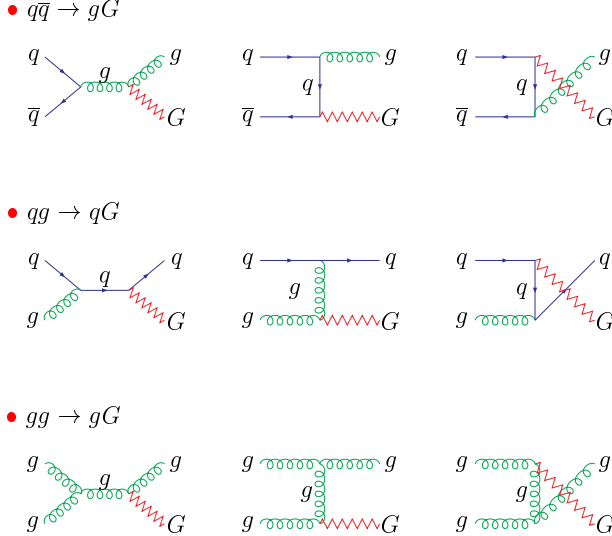


FIG. 1: Lowest-order Feynman diagrams for the emission of real gravitons in $p\bar{p}$ collisions.

10 fm, respectively.

All the states in the KK graviton tower, including the massless state, couple in an identical manner with universal strength of M_{Pl}^{-1} . However there are $(ER)^n$ massive KK modes that are kinematically accessible in a collider process with energy E . The sum over the contribution from each KK state removes the Planck scale suppression and replaces it by powers of the fundamental scale $M_D \sim \text{TeV}$. The interactions of the massive KK graviton modes can then be observed in collider experiments either through their direct production and emission or through their virtual exchange in standard model processes [5].

There are three processes in $p\bar{p}$ collisions that can result in the emission of a graviton and a hadronic jet: $q\bar{q} \rightarrow gG$, $qg \rightarrow qG$, and $gg \rightarrow gG$, where q and g are quarks and gluons and G is the graviton. The lowest-order Feynman diagrams for these processes are shown in Figure 1. The calculation of graviton emission is based on the effective low-energy theory that is valid below the scale M_D . The corresponding Feynman rules are cataloged in [3, 6]. Since the graviton passes through the detector without decaying or interacting, the experimental signature is missing transverse energy (\cancel{E}_T) from the emitted graviton and a hadronic jet from the outgoing quark or gluon.

In this Letter we report the results of a search for the direct production of KK graviton modes using the rate of events with one or two energetic jets and large \cancel{E}_T at the Collider Detector at Fermilab (CDF). The search is based on $84 \pm 4 \text{ pb}^{-1}$ of integrated luminosity recorded with the CDF detector during the 1994–95 Tevatron run.

The CDF detector is described in detail in [7]. The momenta of charged particles are measured in the

central tracking chamber (CTC), which is positioned inside a 1.4 T superconducting solenoidal magnet. Outside the magnet, electromagnetic and hadronic calorimeters arranged in a projective tower geometry cover the pseudorapidity region $|\eta| < 4.2$ [8] and are used to identify jets. Jets are defined as localized energy depositions in the calorimeters and are reconstructed using an iterative clustering algorithm with a fixed cone of radius $\Delta R \equiv \sqrt{\Delta\eta^2 + \Delta\phi^2} = 0.7$ in $\eta - \phi$ space [9]. The transverse energy of a jet is $E_T = E \sin \theta$, where E is the scalar sum of energy deposited in the calorimeter towers within the cone, and θ is the angle formed by the beam-line and the cone axis [10]. For this analysis, jets are required to have $E_T \geq 15 \text{ GeV}$.

The missing transverse energy is defined as the negative vector sum of the transverse energy in the electromagnetic and hadronic calorimeters, $\cancel{E}_T = -\sum_i (E_i \sin \theta_i) \hat{n}_i$, where E_i is the energy of the i -th tower, \hat{n}_i is a transverse unit vector pointing to the center of each tower, and θ_i is the polar angle of the tower. The sum extends to $|\eta| = 3.6$. The data sample was selected with an online trigger that requires $\cancel{E}_T \equiv |\cancel{E}_T| > 30 \text{ GeV}$. This is a sample dominated by instrumental backgrounds and by multijet events, where the observed missing energy is largely a result of jet mismeasurements and detector resolution.

The two-stage preselection we use to reject beam and detector-related backgrounds, beam halo, and cosmic ray events is described in [11]. Events that pass the preselection are then required to have only one or two jets with $E_T \geq 15 \text{ GeV}$, with at least one jet within $|\eta| < 1.1$.

We remove events where the missing energy is due to energy flow from a jet to an uninstrumented region of the detector by requiring that the second highest E_T jet does not point in η to a detector gap if it is within 0.5 radians in ϕ of the \cancel{E}_T direction. We reduce the residual mismeasured multijet backgrounds by requiring that the minimum $\delta\phi$ between the \cancel{E}_T vector and any jet in the event ($\delta\phi_{min}$) is greater than 0.3 radians and the z position of the event vertex is within 60 cm of the nominal interaction point.

To reduce the physics background contribution from electroweak processes with leptons in the final state (dominated by $W(\rightarrow \ell\nu)$) we require that the two highest energy jets are not purely electromagnetic (by requiring the electromagnetic fraction $f_{em} \equiv E_{em}/E_{Tot} \leq 0.9$) and the isolated track multiplicity, N_{trk}^{iso} [12] is zero. For the final sample, we require $\cancel{E}_T \geq 80 \text{ GeV}$, $E_T \geq 80 \text{ GeV}$ for the leading jet and $E_T \geq 30 \text{ GeV}$ for the second jet if there is more than one jet in the event. By accepting events with an energetic second jet we can reliably normalize the background predictions from QCD simulation using the jet data, control the systematic uncertainty on the signal due to initial/final state radiation (ISR/FSR),

TABLE I: The data selection path for the \cancel{E}_T plus one or two jets search.

Selection Requirement	Events Passing
Pre-Selection	300945
$1 \leq N_{jet} \leq 2$ (cone 0.7, $E_T \geq 15$ GeV)	
$ \eta (1 \text{ or } 2) < 1.1$	157035
2nd jet gap veto	
$\delta\phi_{min} \geq 0.3$	
$ z_{vertex} \leq 60$ cm	50938
$f_{em}(1), f_{em}(2) \leq 0.9$	21012
$N_{trk}^{iso}=0$	16459
$E_T(1) \geq 80$ GeV	
If $N_{jet} = 2, E_T(2) \geq 30$ GeV	897
$\cancel{E}_T \geq 80$ GeV	284

and interpret the results with a K -factor (the ratio of the cross sections at leading-order (LO) and next-to-leading-order (NLO), $K = \sigma_{NLO}/\sigma_{LO}$) included in the estimated signal cross section.

The selection requirements and the number of events passing at each stage are summarized in Table 1.

Background events with missing energy and one or two jets arise from standard model sources, predominantly $Z(\rightarrow \nu\bar{\nu})+\text{jets}$, $W(\rightarrow \ell\nu)+\text{jets}$ ($\ell = \tau, \mu, e$), and residual QCD production. While $Z(\rightarrow \nu\bar{\nu})+\text{jets}$ produces real $\cancel{E}_T+\text{jets}$, $W(\rightarrow \ell\nu)+\text{jets}$ mimics our signal when the lepton is lost or misidentified. To estimate the $Z+\text{jets}$ and $W+\text{jets}$ background levels and their uncertainties in the final sample we normalize PYTHIA [13] Monte Carlo (MC) predictions using the observed $Z(\rightarrow e^+e^-)+\text{jets}$ data sample. QCD dijet events mimic our signal when one jet is badly mis-measured, resulting in large \cancel{E}_T . For the QCD predictions we use the HERWIG MC program [14] and normalize to the high statistics jet data samples using well-balanced dijet events. We estimate additional backgrounds from $t\bar{t}$, single top and diboson production using MC predictions [13, 14], which we normalize using the respective theoretical cross section calculations for these processes [15].

The predicted backgrounds from standard model processes are summarized in Table 2. Of the 274 total events predicted to pass our selection requirements, 160 are predicted to come from $Z(\rightarrow \nu\bar{\nu})+\text{jets}$, 89 from the combined $W(\rightarrow \ell\nu)+\text{jets}$ electroweak processes, and 22 from QCD production. Because the MC predictions have been normalized to high statistics data samples, the dominant uncertainty on the $W+\text{jets}$ and $Z+\text{jets}$ predictions is the 4% luminosity uncertainty. The QCD prediction has an additional 14% uncertainty due to jet energy resolution [11]. We observe 284 events in the data. In Figure 2 the predicted standard model \cancel{E}_T distribution is compared

TABLE II: The predicted number of events in the final sample from standard model sources and the number observed in the data.

Background Source	Predicted Events
$Z(\rightarrow \nu\bar{\nu})+\text{jets}$	160.2 ± 11.5
$W(\rightarrow \tau\nu)+\text{jets}$	46.6 ± 5.5
$W(\rightarrow \mu\nu)+\text{jets}$	23.8 ± 5.0
$W(\rightarrow e\nu)+\text{jets}$	18.1 ± 4.3
QCD	21.7 ± 6.7
$t\bar{t}$, single t , dibosons	3.9 ± 0.3
Total predicted	274.1 ± 15.9
Observed	284

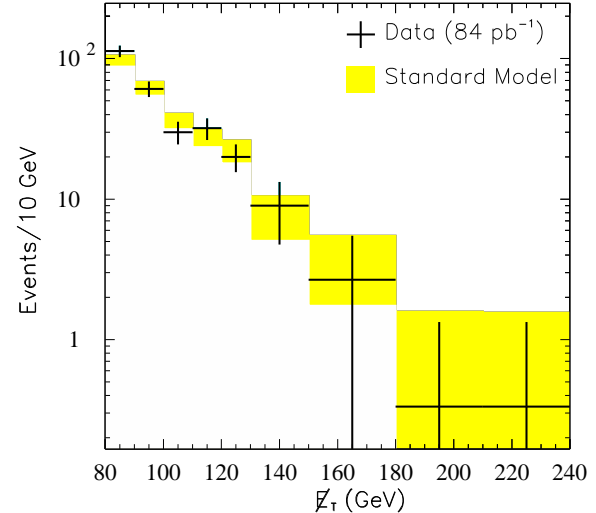


FIG. 2: Comparison between data (points) and standard model predictions (boxes) of the \cancel{E}_T distribution. There are 284 data events, to be compared with 274 ± 16 events predicted from standard model sources. The distribution is plotted with a variable bin size; the contents for bin sizes greater than 10 GeV are normalized accordingly. The height of the boxes shows the uncertainty on the standard model prediction.

with the distribution we observe in the data. In Figure 3 the same comparison is shown for other kinematic distributions. In both figures the data are consistent with the expected background. An additional contribution from graviton production would result in a smooth excess over the background in nearly all the kinematic distributions, as shown in Figure 4 for \cancel{E}_T .

We use the PYTHIA MC program to generate datasets of graviton emission, using the leading-order production cross sections calculated in [3]. The signal

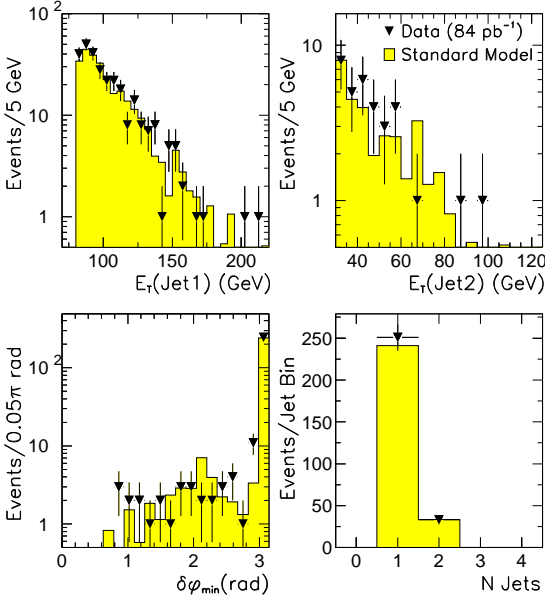


FIG. 3: Comparison between data (points) and standard model predictions (histogram) of the first and second leading jet E_T , $\delta\phi_{\min}$, and N_{jets} distributions.

processes are simulated for $n = 2, 4$, and 6 extra dimensions, and for a range of values of M_D . The signal efficiency ranges from 2.9% for two extra dimensions to 6.4% for six extra dimensions (due to different relative weights of the three production processes of Figure 1) and is largely independent of M_D . The total relative systematic uncertainty on the signal efficiency is 25% , mostly due to modelling of ISR/FSR (21%), jet energy scale (11%), renormalization scale (8%) and parton density functions (2%) [16].

Using a Monte Carlo technique to convolute the uncertainty on the background estimate with the relative systematic uncertainty on the signal efficiency, the 95% C.L. [17] upper limit on the number of signal events is 62 . As shown in Figure 5, for $K = 1.0$ we exclude an effective Planck scale less than 1.00 TeV for $n = 2$, less than 0.77 TeV for $n = 4$, and less than 0.71 TeV for $n = 6$. Recently the D0 collaboration reported a limit on direct graviton emission using a K -factor of 1.3 in the signal cross section [18]. They report limits of 0.99 TeV for $n = 2$, 0.73 TeV for $n = 4$ and 0.65 TeV for $n = 6$. For direct comparison, using $K = 1.3$ our corresponding lower limits on M_D are 1.06 TeV for $n = 2$, 0.80 TeV for $n = 4$, and 0.73 TeV for $n = 6$.

These are the best limits to date on direct graviton emission [18, 19] from the Tevatron.

Assuming compactification on a torus, the limits on M_D with $K = 1.0$ correspond to limits on the compactification radius of $R < 0.48$ mm for $n = 2$,

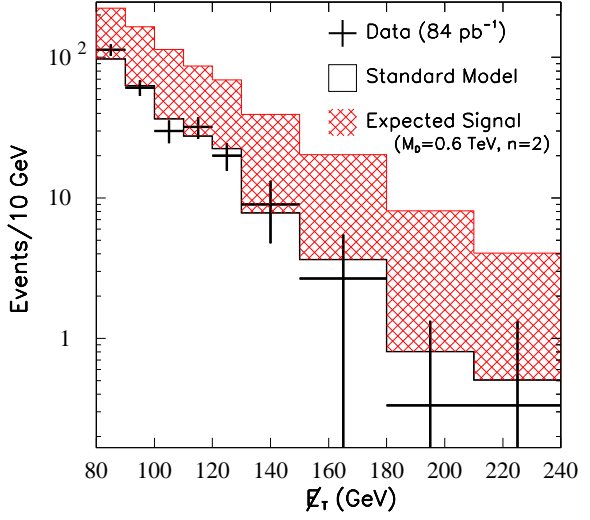


FIG. 4: The predicted \not{E}_T distribution from standard model processes (histogram) and the one from the expected graviton signal (for $n = 2$, $M_D = 0.6$ TeV, and a K -factor of 1.0) added to the standard model (hatched). The signal appears as a smooth excess over the standard model background. The points are the observed data.

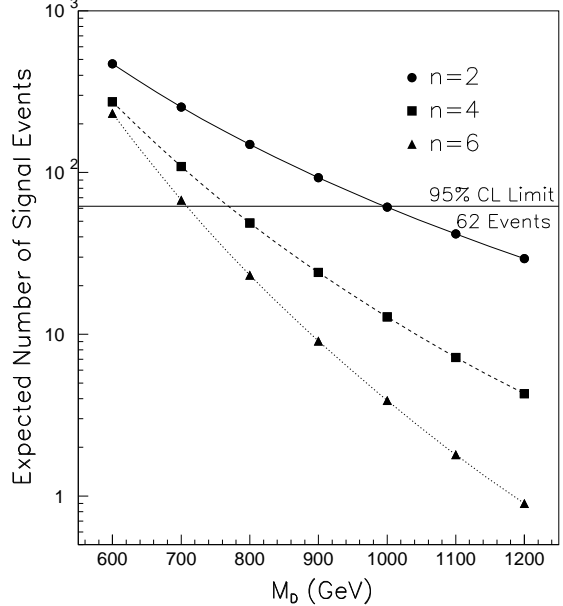


FIG. 5: The three curves show the number of expected signal events for $n = 2, 4$, and 6 extra dimensions as a function of the effective Planck scale M_D for a K -factor of 1.0 . The straight line shows the 95% C.L. upper limit on the number of signal events.

$R < 0.014$ nm for $n = 4$, and $R < 42$ fm for $n = 6$.

We thank the Fermilab staff and the technical staffs of the participating institutions for their vital contributions. This work was supported by the U.S. Department of Energy and National Science Foundation; the Italian Istituto Nazionale di Fisica Nucleare; the Ministry of Education, Science, Sports and Culture of Japan; the Natural Sciences and Engineering Research Council of Canada; the National Science Council of the Republic of China; the Swiss National Science Foundation; the A. P. Sloan Foundation; the Bundesministerium fuer Bildung und Forschung, Germany; the Korea Science and Engineering Foundation (KoSEF); the Korea Research Foundation; the Comision Interministerial de Ciencia y Tecnologia, Spain; and the Pritzker Foundation. We thank Konstantin Matchev and Joe Lykken for providing the MC generation code for graviton production in $p\bar{p}$ collisions [20].

imuthal and polar angles with respect to the proton beam direction. The pseudorapidity η is defined as $\ln[\tan(\theta/2)]$.

- [9] F. Abe *et al.*, CDF Collaboration, Phys. Rev. **D45**, 1448 (1992).
- [10] If there are multiple vertices in the event we use the vertex with the largest $\sum P_T$ of associated tracks.
- [11] T. Affolder *et al.*, CDF Collaboration, Phys. Rev. Lett. **88**, 041801 (2002).
- [12] N_{track}^{iso} is the number of high momentum isolated tracks in the event. Tracks qualify as such if they have transverse momentum $P_T \geq 10$ GeV/c, impact parameter $d_0 \leq 0.5$ cm, vertex difference $|z_{track} - z_{event}| < 5$ cm and the total transverse momentum ΣP_T of all tracks (with impact parameter $d_0 \leq 1$ cm) around them in a cone of $\Delta R \equiv \sqrt{\Delta\eta^2 + \Delta\phi^2} = 0.4$ is $\Sigma P_T \leq 2$ GeV/c.
- [13] T. Sjöstrand, Comput. Phys. Commun. **82**, 74 (1994). PYTHIA v6.115 is used.
- [14] G. Marchesini *et al.*, Comput. Phys. Commun. **67**, 465 (1992). HERWIG v5.6 is used. See hep-ph/9607393 (1996).
- [15] R. Bonciani *et al.*, Nucl. Phys. **B529**, 424 (1998); T. Stelzer, Z. Sullivan and S. Willenbrock, Phys. Rev. **D54**, 6696 (1996); T. Tait and C. P. Yuan, hep-ph/9710372 (1997); J. Ohnemus *et al.*, Phys. Rev. **D43**, 3626 (1991); Phys. Rev. **D44**, 1403 and 3477 (1991); T. Affolder *et al.*, Phys. Rev. **D64** 032002 (2001).
- [16] MRSD- is used as our reference structure function; A. D. Martin, W. J. Stirling and R. G. Roberts, Phys. Rev. **D47**, 867, (1993).
- [17] G. Zech, Nucl. Instrum. Methods **A277**, 608 (1989); T. Huber *et al.*, Phys Rev **D41**, 2709 (1990).
- [18] V. M. Abizov *et al.*, D0 collaboration, Phys. Rev. Lett. **90**, 251802 (2003).
- [19] D. Acosta *et al.*, CDF Collaboration, Phys. Rev. Lett. **89**, 281801 (2002). For a summary of LEP results on graviton emission, see G. Landsberg, “*Extra Dimensions and More*,” [arXiv:hep-ex/0105039].
- [20] The current version of PYTHIA(6.2) includes these processes. T. Sjöstrand, P. Edén, C. Friberg, L. Lönnblad, G. Miu, S. Mrenna and E. Norrbin, Comput. Phys. Commun. **135**, 238 (2001).

-
- [1] G. Nordstrom, Z. Phys. **15**, 504 (1914); T. Kaluza, Preuss. Akad. Wiss., Berlin, Math. Phys. K **1**, 966 (1921); O. Klein, Z. Phys. **37**, 895; Nature **118**, 516 (1926).
 - [2] N. Arkani-Hamed, S. Dimopoulos and G. R. Dvali, Phys. Lett. B **429**, 263 (1998).
 - [3] G. F. Giudice, R. Rattazzi and J. D. Wells, Nucl. Phys. B **544**, 3 (1999).
 - [4] Steven Weinberg Phys. Lett. B **82**, 387 (1979); Eldad Gildener Phys. Rev. D **14**, 1667 (1976).
 - [5] E. A. Mirabelli, M. Perelstein and M. E. Peskin, Phys. Rev. Lett. **82**, 2236 (1999). For a review, see J. Hewett and M. Spiropulu, Ann. Rev. Nucl. Part. Sci., Vol. **52**: 397-424 (2002).
 - [6] T. Han, J. D. Lykken and R. J. Zhang, Phys. Rev. D **59**, 105006 (1999) [arXiv:hep-ph/9811350].
 - [7] F. Abe *et al.*, Nucl. Inst. and Methods, **A271**, 387 (1988).
 - [8] In the CDF coordinate system, ϕ and θ are the az-